CDW aluminium joints welding and optimisation with NDT/mechanical testing

Francesco W. Panella, Vito Dattoma, Marta De Giorgi, Fania Palano & Alessio Carofalo

The International Journal of Advanced Manufacturing Technology

ISSN 0268-3768

Int J Adv Manuf Technol
DOI 10.1007/s00170-019-03412-y

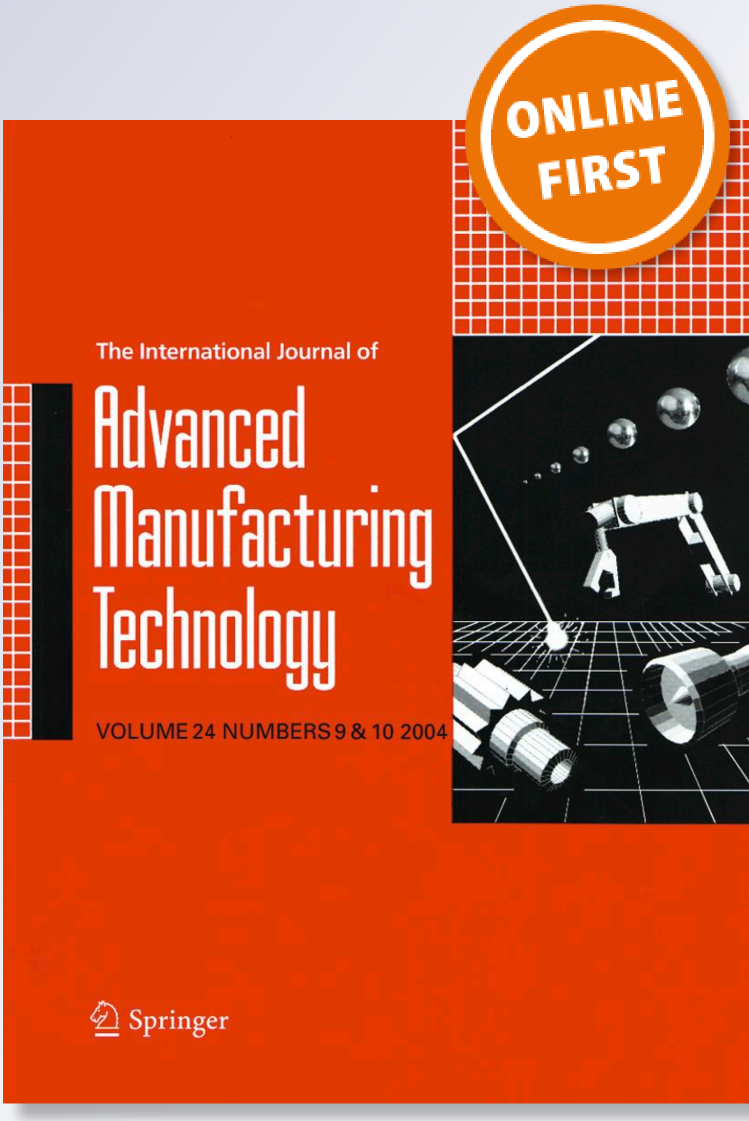

The International Journal of Advanced Manufacturing Technology
https://doi.org/10.1007/s00170-019-03412-y

ORIGINAL ARTICLE

CDW aluminium joints welding and optimisation with NDT/mechanical testing

Francesco W. Panella[1] · Vito Dattoma[1] · Marta De Giorgi[1] · Fania Palano[2] · Alessio Carofalo[1]

Received: 12 November 2018 / Accepted: 29 January 2019

Abstract

This work investigates the possibility to apply the improved hybrid capacitor discharge welding (CDW) process, based on projection welding principles, to aluminium alloy Al 5754. The CDW process is an electrical resistance welding technology, realised with high-intensity current pulses discharged by large capacitors. The innovative aspect is the effective possibility to weld aluminium alloys with CDW process and improve the mechanical weld characteristics and the presence of defects as a function of the technological parameters; intrinsic CDW process characteristics need to be investigated on the basis of interaction between the technological and geometrical aspects and the related mechanical properties, in order to improve welding shape and reduce defect size. In order to optimise the process, visual and ultrasonic inspections of the most significant welded joints were performed, and residual stress values were checked; in addition, high-cycle fatigue tests after room temperature tensile tests were executed to optimise the weldments.

Keywords Capacitor discharge welding · Welded joints · Al 5754 · Fatigue tests · Ultrasonic test · Residual stress

1 Introduction

The capacitor discharge welding (CDW) process is an electrical resistance welding technology realised through intense current pulses discharged by great capacitor banks. This process allows the production of low stress concentration at the weld toe and allows obtaining thin sound welds and good material integrity [1, 2].

The CDW process is currently applied in automotive industry applications, offering rapid and repetitive butt welding of pulley, gears and cable head junctions in engine and mechanism assemblies.

The present paper deals with new developments of the CDW process, referred particularly to aluminium alloy 5057 butt joints, with the principal aim to study the process characteristics, to analyse the resultant mechanical behaviour and to verify the presence of defects, in order to improve the weld properties.

The main CDW parameters (energy input, applied forces and igniter dimensions) were optimised for Al 5057 butt joints, given the novel tool to weld jointed sections wider than 60 mm^2, never obtained with CDW methods. Critical process characteristics are the contact conditions as a function of pressure between the parts and number of discharges at different power inputs, as well as the electrodes gripping system [3].

A second innovative aspect is the modification of the igniting point geometry [4] on the section to be welded and optimise new weld characteristics; the goal is to impose the local fusion processes more uniformly on the whole area and enhance the weld properties. Innovative trapezoidal contact geometry with suited welding parameters was studied on the basis of the previous work [5] where CDW simulations were performed.

This research focuses the attention on the multipoint CDW (MCDW) technique conceived by the authors, which represents a hybrid process between the capacitor discharge welding and projection welding [6, 7]. It is proposed with the aim to join larger surfaces and free from defects typical of CD welds, such as porosity and lack of fusion.

In this work, butt-weld rectangular section specimens are machined to adopt a trapezoidal contact profile on one of the parts to be welded.

✉ Francesco W. Panella
francesco.panella@unisalento.it

[1] Department of Engineering for Innovation (DII), University of Salento, Lecce, Italy

[2] SSPT-PROMAS-MATAS, ENEA C.R. Brindisi, SS 7 km 706, 72100 Brindisi, Italy

Published online: 22 February 2019

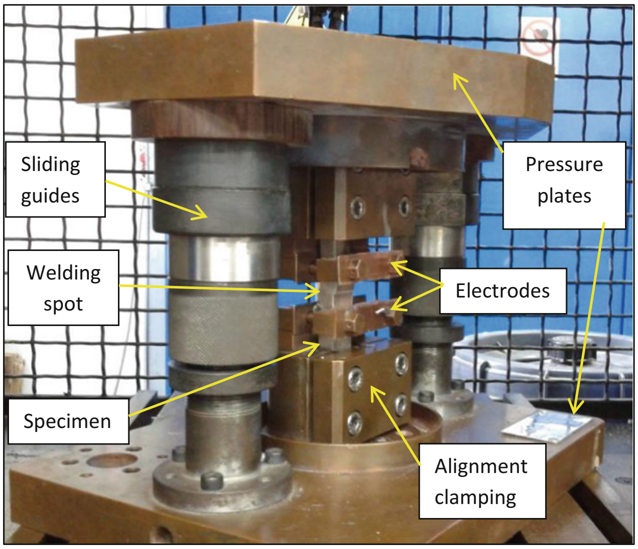

Fig. 1 Welding equipment with welded specimens gripped in the centre

The static and fatigue properties were subsequently analysed for the welded joints, and the results were correlated to process parameters, in order to enhance the process for repair purposes of industrial components, despite the fact that some brittle character was observed for the welded joints. Static tests produced good results with respect to base metal, if the proper welding parameters are settled; these tests were performed on joints realised with different applied energy, identifying the optimal process configuration. The efficiency of the CDW technique in terms of repeatability and welded product quality has to be guaranteed for future applications; consequently, fracture section analysis of best-welded specimens was scheduled, and residual stresses were also measured, to confirm the optimal welding parameters and welding bead homogeneity. Residual stress measurements were performed by means of the hole-drilling method, according to ASTM E837-01 standards in order to evaluate the significant presence of stresses beside the CD weld bead.

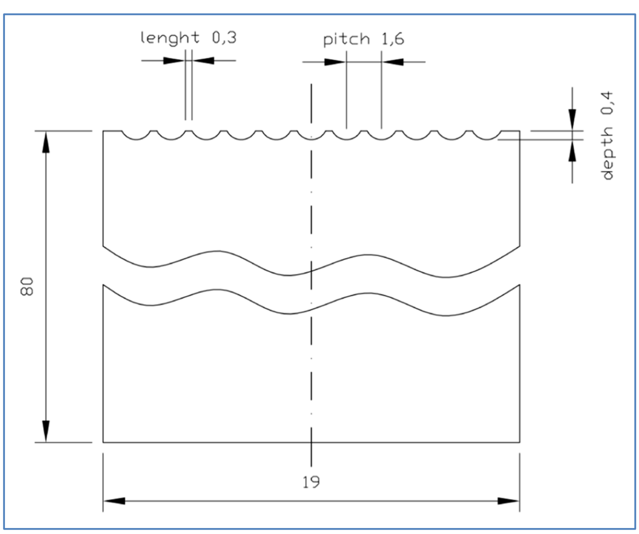

Fig. 2 Trapezoidal profile for the joints

At last, the weld quality in terms of the presence of defects was analysed by means of ultrasonic inspections and finally fatigue tests were performed, according to ND control validation on specimens, obtaining a reduced presence of defects [8].

2 Materials and methods

The MCDW process consists of rapid and elevated intensity current flow discharged onto small igniters, positioned between the parts to be welded [3]; igniter material is partially fused and transformed in plasma state by intensive Joule effect, allowing to melt narrow layers of base metal in the proximity of joining surfaces and to achieve the complete weld with the contemporaneous aid of compression forging forces [2].

This way, the process offers rapid cooling rates in the order of 10^6 K/s or more, typical of electron beam welding or laser welding, among alternative technologies [9]; it is also worth pointing out that the welding profile deformations induced by this process are negligible, reducing the subsequent machining and control costs.

According to authors' works [3, 4] and in relation to scientific literature data [2], small-diameter welded bars can be easily achieved up to 6 mm with cylindrical single igniter geometry. For wider surfaces, more igniting points such as the multipoint trapezoidal contact profile have to be used. The multipoint version of the CDW has been experimented in order to produce a sound weld and ensure a more uniform process on the whole section.

The welded joints have been realised by means of a capacitor discharge welding machine Daiko TDA. Large capacitor banks (8320 F) at high voltage are connected to discharging pulse transformers, producing suitable current flowing in the secondary welding circuit working at 10–15 V, to be applied on welding specimens.

In order to perform CDW multipoint process on rectangular section specimen, dedicated welding equipment was conceived and fabricated; several aspects have to be improved, such as a better specimen clamping into the machine, the application of calibrated loads and the perfect alignment and grip with enhanced electrical continuity at the electrodes (Fig. 1). In addition, the tools include an adjustable contrast system to be fixed to the specimen axis,

Table 1 Example of pre-heating process cycle, to be applied before welding

F [daN]	E_1 [J]	E_2 [J]	E_3 [J]	E_4 [J]	E_5 [J]	I_p [kA]
3000	2000	3000	4000	5000	6000	72

Table 2 Input parameters and welding outcome for the first set of welded specimens

Specimen	F [daN]	E_1 [J]	E_2 [J]	E_3 [J]	E_4 [J]	E_5 [J]	I_p [kA]	I_i [C]
1	2500	2000	4000	6000	8000	10,000	n.d.	n.d.
2	3000	2500	5000	5000	18,000	5000	156	953
3	3000	2500	4000	4000	20,000	10,000	156	963
4	2500	2500	4000	6000	22,000	15,000	156	911
5	2000	2500	4000	6000	22,000	15,000	156	606
6	2000	2500	4000	8000	20,000	25,000	156	882
7	2000	3000	6000	10,000	25,000	35,000	156	571
8	2500	3000	6000	8000	12,000	25,000	156	984
9	2500	4000	8000	12,000	25,000	15,000	156	943
10	2500	4000	8000	15,000	25,000	25,000	156	1010
11	2500	4000	8000	15,000	30,000	15,000	156	917
12	3000	4000	8000	12,000	25,000	15,000	156	920
13	3000	4000	8000	12,000	30,000	15,000	156	920
14	2500	4000	8000	12,000	30,000	15,000	156	930
15	2500	2500	4000	8000	20,000	25,000	156	930
16	2000	2500	4000	8000	15,000	25,000	156	887
17	2500	2500	4000	8000	15,000	30,000	156	909

in order to limit and control the welding depth and consequently material deformation.

In this work, the CDW process is applied to weld aluminium alloy 5754 in butt-weld rectangular samples having a section width of 19 mm and depth 9 mm; specimens were machined to adopt a small trapezoidal contact profile, as described in Fig. 2.

3 Welding experiments and results

3.1 Welding tests

Up to now, no data besides the authors [5, 7] concerning weld characteristics and fatigue behaviour of the CD Welded aluminium joints are present in scientific literature; from these studies, it can be deduced that few defects such as porosity and lack of welding uniformity are present, and repeatability is critical, since the process can be unstable due to electro-mechanical interactions. It was decided to experiment CDW aluminium specimens, using a large number of specimens to select the best welding parameters and enhance the weld characteristics; the aluminium alloy 5754 is an aluminium-magnesium alloy, easy to be fusion welded and no heat

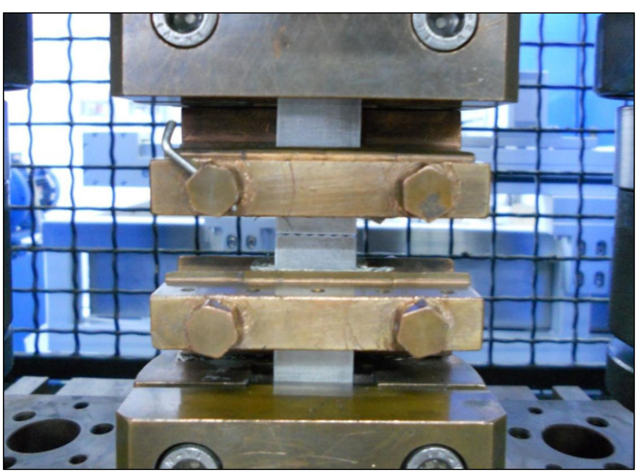

Fig. 3 Specimen assembled in the welding equipment

Table 3 Input parameters for the best welded specimens

Specimen	F [daN]	E_1 [J]	E_2 [J]	E_3 [J]	E_4 [J]	E_5 [J]
18	2500	4000	8000	12,000	25,000	15,000
19	2500	2500	4000	8000	15,000	30,000
20	2500	2500	4000	8000	15,000	30,000
21	2500	4000	8000	12,000	25,000	15,000
22	2500	4000	8000	12,000	25,000	15,000
23	2500	2500	4000	8000	15,000	30,000
24	2500	2500	4000	8000	15,000	30,000
25	2500	2500	4000	8000	15,000	30,000
26	2500	2500	4000	8000	15,000	30,000
27	2500	3000	6000	10,000	15,000	30,000
28	2500	2500	4000	8000	15,000	30,000
29	2500	3000	6000	10,000	15,000	30,000
30	2500	3000	6000	10,000	15,000	35,000
31	2500	3000	6000	10,000	15,000	35,000
32	2500	3000	6000	10,000	15,000	30,000
33	2500	3000	6000	10,000	15,000	30,000

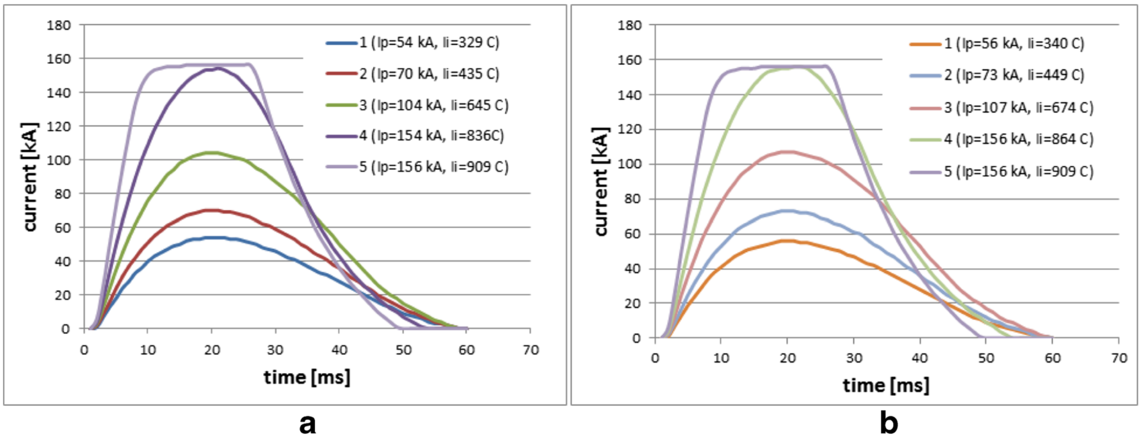

Fig. 4 Discharged current intensity for the five measured pulses on specimens 16 (**a**) and 17 (**b**)

treatments were done on the parts prior and after welding, whilst a gas shielding transparent chamber with Argon was used to prevent oxidation during process.

The test welding session was performed in two phases: firstly, several welding parameter sets were studied and secondly, the parameters that produced the best welds in terms of mechanical properties were selected to weld other specimens for deeper investigations. This way, the characteristics of the joints welded with the same parameters are compared, in order to verify results repeatability.

In the first welding session, the process parameters were modified from time to time on the bases of previous works and available numerical data; the energy was furnished in five discharges; in Tables 1 and 2, the input parameters, employed in each discharge and the output welding outcome given by the machine are summarised for all specimens with the following significance of abbreviations: *F* the compressive force applied; E_i the electrical energy of the *i*th discharge; I_p the maximum current peak; I_i is the integrated current over time. In Table 1, the pre-heating process cycle, to be applied before welding to set the specimens into grips and improve initial contact state, is described.

According to Table 2, the fundamental discharge is only the fourth or the fifth one and occasionally the third one; since a single discharge of maximum power is insufficient, other discharges have lower intensity for pre-heating purposes. All specimens were welded by applying a force in the range 20–30 kN.

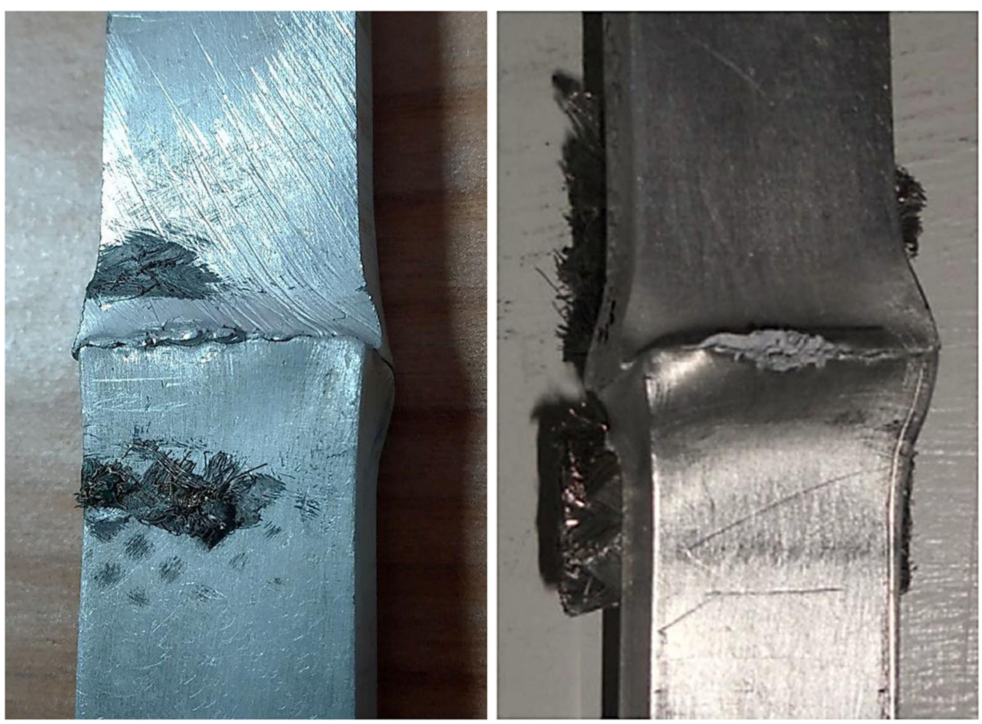

Fig. 5 Welded specimens example nos. 13 and 17 after welding

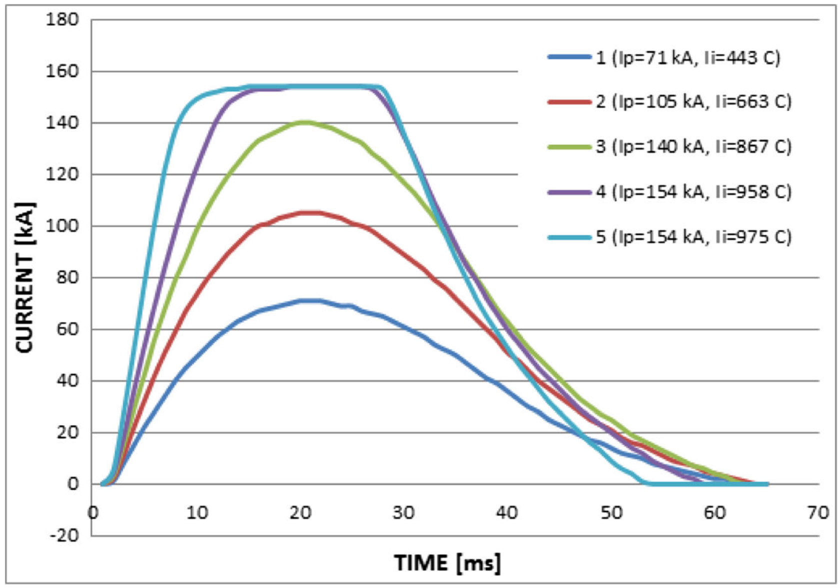

Fig. 6 Discharged current intensity for the five measured pulses on specimen 33

The presence of alumina oxide superficial layer on specimens, which interferes with the welding process [10–13], has to be manually removed before welding and specimens have also to be cleaned. Special spacers must also be used to correctly place the specimens into grips, in order to assure geometrical stability for each specimen and reduce angular misalignments between the parts; copper tinned flexible spacers are selected and placed on specimen sides to better house it into grips and assure the optimal conductivity (Fig. 3). During the welding tests, it can be observed that the applied force on the specimen is directly proportional to the electric discharge value, according to diminished contact resistance.

In some cases, i.e. specimen 5 welded with force 2000 daN and electrical discharge 22,000 J, the specimen resulted burned because the low force level does not guarantee sufficient contact and avoid electrical arc to occur; the same phenomenon was verified for specimen 7 and 14. In some cases, igniter explosion occurs, due to electric arc strikes; it must be avoided not only to obtain good welds, but also because it damages the electrode surface with some aluminium inclusions.

The first welding trials revealed the importance of specimen pre-heating (Table 1), realised with a preliminary welding prescribed cycle, characterised by low-value discharges and aiming also to warm the contact spots before fusion takes place. The discharged current intensity diagrams are reported as follows for the best-welded specimens, in order to control the current peak I_p limit values and modify the technological parameters for successive welding tests.

Tensile test results were used to compare different welded specimens; it can be deduced that the optimal parameters are to be referred to welded specimens 9 and 17 (Table 3 and Fig. 4).

Table 4 Uniaxial tension test results

Specimen test number	Area$_I$ [mm^2]	Maximum load [kN]	Elongation [%]	UTS [MPa]
2	184.8	22.0	0.30	119
4	171.0	25.5	9.61	149
6	184.8	42.8	5.72	232
7	192.6	19.5	0.48	101
9	183.8	49.2	13.99	267
10	171.0	6.0	2.27	35
11	185.3	22.8	3.09	123
12	183.8	13.3	0.11	73
13	184.1	28.9	10.33	157
14	188.2	19.2	0.58	102
16	185.8	39.0	5.10	210
17	187.5	51.5	4.43	275
18	184.8	36.4	4.60	197
19	187.5	44.2	6.44	236

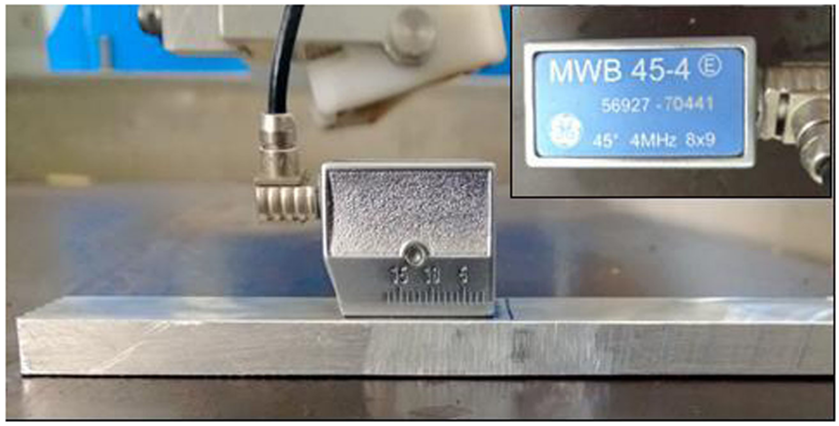

Fig. 7 Selected Ultrasonic probe MWB 45-4, as applied on the welded specimen

These welds seem to be optimal; reduced volume expulsed from the weld is observed with small part distortion and the weld bead seems to be homogeneous in shape and thickness around the welded profile, as previously achieved with multipoint contact CDW studies [5].

According to these results, a second series of welding tests was planned and executed on the bases of technological parameters referred to specimens 9 and 17 (Fig. 5); further, small changes were included: from specimens 30, two pre-heating cycles were used and the welding discharge ramp was slightly modified in such a way to increase the energy raise before the final discharge, as visible by the parameters in Table 3. These changes seem to produce a thicker weld bead and the increase of weld penetration depth, considered as a reliable indicator of welding quality [7].

Good welds were found in specimens 24–28, characterised by optimal weld aspect, but small penetration depth values. Specimens 27–29 produced better alignment and depth results, indicating that good fusion takes place in the welded volume, whilst specimen 30 was welded with higher energy input in similar conditions and different gripping spacers. All results were not easy to be interpreted, especially considering that an energy limit exists, above which the specimens may explode (as for specimen 31, $E_{max} = 35{,}000$ J). A good compromise seems to bring force and energy values the highest as possible before mechanical and electrical collapse occurs. For this reason, the use of pre-heating cycles before welding seems crucial, as well as good specimen mounting operations are proved to be very influent on the final result; they need to be carefully done and standardised.

Last welding tests on specimens 32 and 33 produced the optimal results. In Fig. 6, the discharged current is displayed for the specimen 33, showing a large integral area I_i and a considerably high peak level, without reaching the input parameter limit values previously described. For these joints, the weld bead showed the optimal shape, i.e. the thicker, constant and coherent bead around the weld line.

3.2 Uniaxial tests

The uniaxial tension tests were performed to determine the mechanical properties of the welded material. This data showed the reference values for the successive fatigue tests on welded specimens.

Table 5 ND test results after ultrasonic scanning on both specimen sides

No.	Amplitude [%]	Signal level peak [%]	% dB damage range	Approximate lateral extension [mm]	Severity
20	8.5	87	> − 6 dB	10	High
21	8.5	85	< − 6 dB	14	Medium
28	8.5	98	− 6 dB	12	Medium
25	− 1.5	98	> + 3 dB	12.5	High
22	− 1.5	100	> + 3 dB	13	High
23	− 1.5	70	0 ÷ + 3 dB	10	High
32	3.0	70	− 6 dB ÷ − 3 dB	8	Low
26	0.5	98	0 ÷ + 3 dB	9	High
27	0.5	63	− 3 dB ÷ 0	8	Low
33	2.5	45	< − 6 dB	Small spot defects	Low
30	2.5	54	− 6 dB ÷ − 3 dB	7	Low

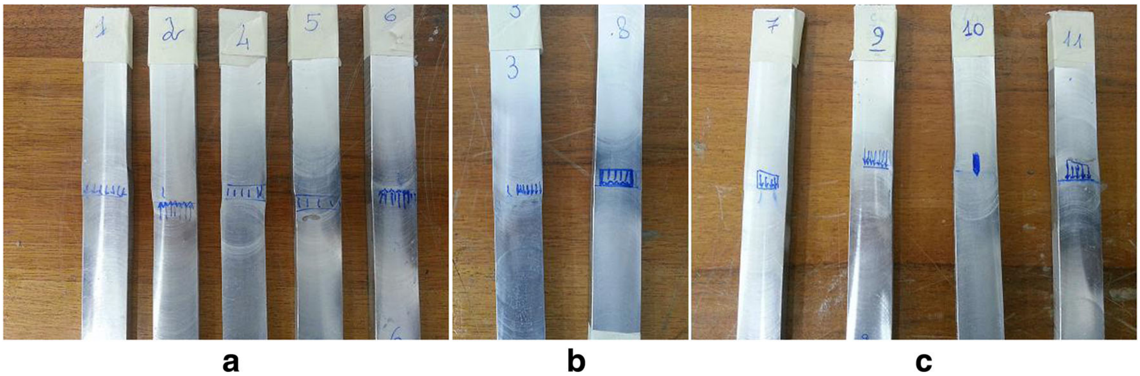

Fig. 8 Classification in three different classes of specimens. **a** Large defects, **b** medium-size presence, **c** small defects

The tests were executed according to the ASTM E8M-0425, that is the standard for room temperature tensile tests.

Testing machine was Instron axial-torsional one endowed with 250-kN load cell. Tests were performed in displacement control mode with 0.5 mm/min translation speed of axial actuator. Fourteen uniform rectangular specimens were tested.

The longitudinal strain of the specimen was estimated with an extensometer. The control unit allowed the verification of the extensometer signal and the computation of the specimen strain during the whole test. In this experimental analysis, the mechanical parameters, like maximum load, ultimate tensile stress and elongation at break, were evaluated (data reported in Table 4).

3.3 UT control procedures

The ND control allows the detection of internal defects, whose size is critical for the welded specimen testing. In particular, UT method allows the detection of the position and size of defects with simple instruments and proper commercial probes for thin welded parts. In this work, the selected probe

Fig. 9 Qualitative A-scans in terms of amplitude percentage. **a** Specimen no. 25 with high indication of defect area, **b** specimen no. 20, medium-size defect, **c** specimen no. 33 with typical small sparse defects

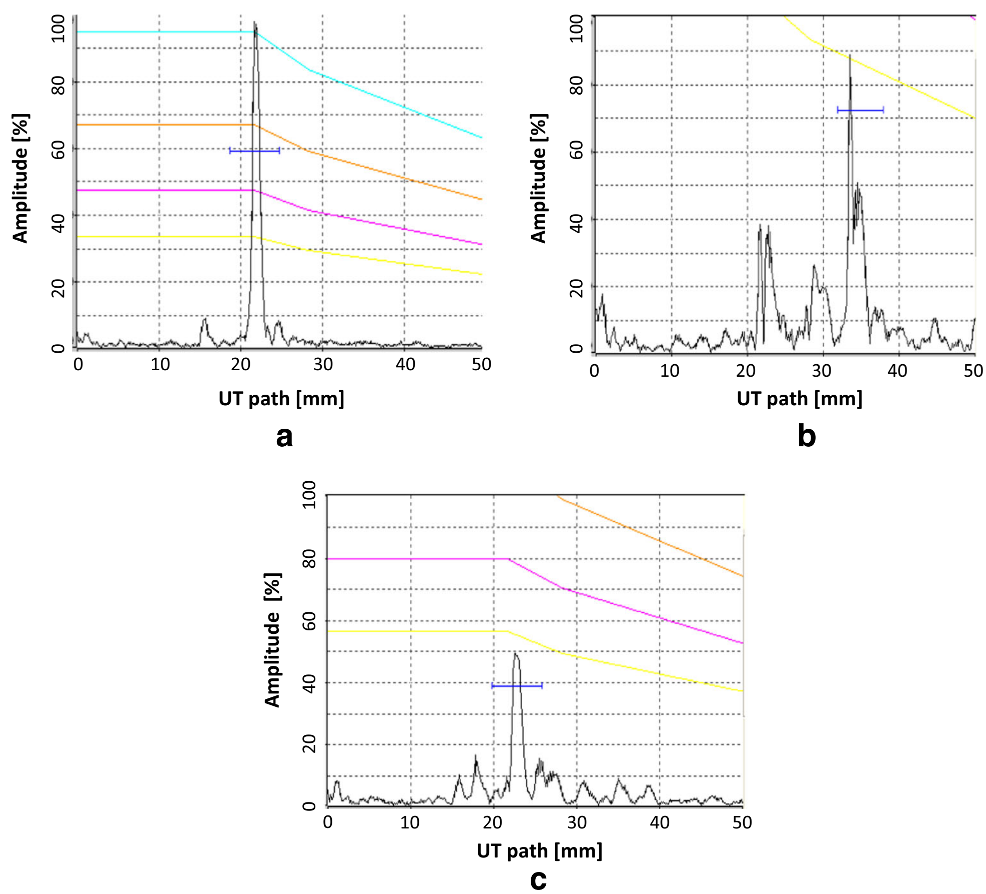

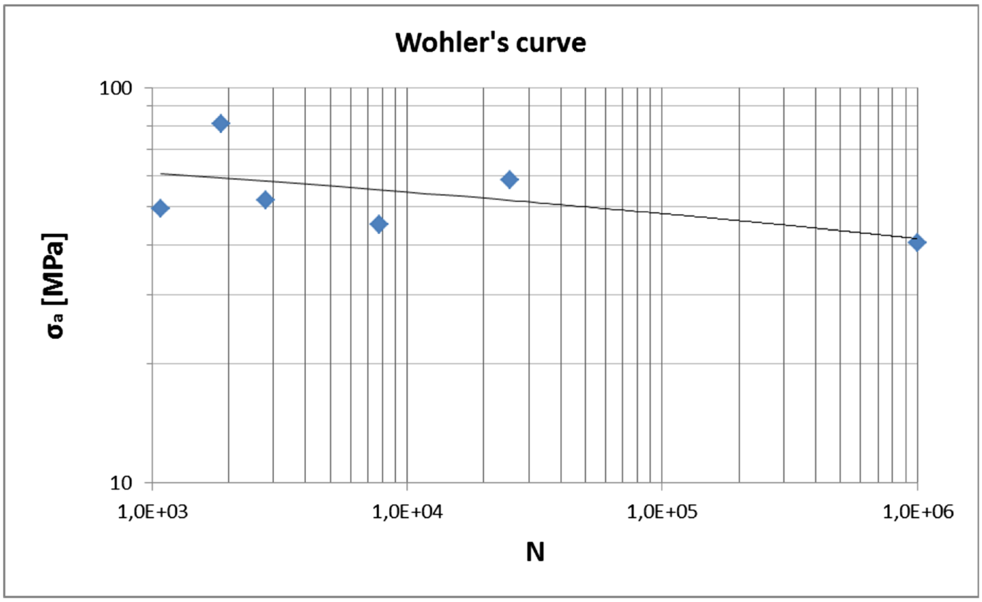

Fig. 10 The Wohler curve of CDW specimens in Al alloy

was MWB 45-4 with integrated wedge (Fig. 7). It represented a classical contact angle beam sensor with a 45° deflection angle and 4-MHz emission frequency.

The G.E. USIP 40 system with suitable software was used for specimen scanning, adopting standard procedures for welded butt joints with a unique transmitter/receiver probe for pulse-echo method, with output data displayed as A-scan diagrams.

Specimens were prepared by levelling the external prismatic surfaces, in order to cut out the CD welding typical slags and locate the probe in maximum proximity of the thin weld bead. Defect severity selection is based on the magnitude of the signal of defect as a function of depth or distance, by comparison with reference distance amplitude correction curves (DAC curve), achieved with artificial defect measurements on similar material; DAC curves were obtained from a metallic sample where 3-mm artificial defects were produced and analysed with specific signal gain according to the defect depth. The curves were representative of different defect conditions: 80% of the reference signal and two curves at − 3 dB and at − 6 dB below the previous one, typically used to determine dangerous defects; also a + 3-dB curve is reported to represent large-size defects. The final measurement data, and in particular the defect area extension, are reported in Table 5.

The severity of the single defect is indicated and the specimens are divided into three different groups: group "a" presents small and scattered defects; the second group "2b" shows extensive lack of penetration in the weld bead and the third group "c" with widespread lack of penetration or "cold weld" defect (Fig. 8).

In Fig. 9, three different A-scan examples of ultrasonic inspections are reported; the typical peaks could be clearly identified. In Fig. 9a, the encountered lack of penetration through thickness in weld bead is reported; these defects are distributed along the central section of weld bead; therefore, the defect is classified as critical for the integrity of the component. In Fig. 9b, the specimen shows several small defects, typical of arch welding, but everyone is contained in the area below − 6 dB. Despite the low amplitude of the signal, this specimen is considered in group "b", because defects are sparsely distributed along the welding surface.

Finally, Fig. 9c shows an A-scan of specimen with small sparse defects, included in the group "c" with good welding quality. The good results as for specimen no. 33 could be obtained thanks to optimization processes, based on previous weld tests. Basically, in Al CD welds, a certain level of defectiveness is always present, the size and distribution of which determines the joint behaviour.

The defects having an amplitude smaller than − 6 dB, even if they are extended along the lateral surface, are classified as not relevant, because they are considered as bonding defects during the welding process.

Table 6 Fatigue tests results

N	σ_{max} [MPa]	σ_m [MPa]	σ_a [MPa]	F_m [N]	Fa [N]	Cycles
33	180	99	81	14,256	11,664	1869
32	130	71.5	58.5	10,296	8424	25,362
28	115	63.25	51.75	9108	7452	2806
27	110	60.5	49.5	8712	7128	1087
21	100	55	45	7920	6480	7782
30	90	49.5	40.5	7128	5832	1,000,000

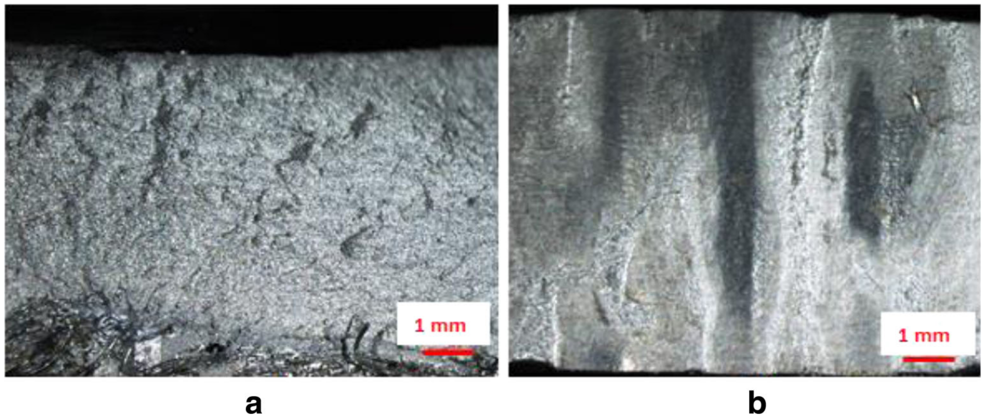

Fig. 11 Fracture surface of specimen no. 33 (**a**) and specimen no. 30 (**b**)

3.4 Fatigue tests

The fatigue Wöhler curve was achieved for the welded specimens (Fig. 10), up to the material limit stresses at 2×10^6 cycles; tests were executed on 8-mm-thick specimens at room temperature. The fatigue tests were performed on welded specimens obtained using the optimal parameters identified in the first step welding and which present low or medium defects, detected by ND-inspection. In total, the tested specimens were six. Despite the small number of specimens, some indications can be clearly observed (Table 6). The specimen no. 33 was tested with a 70% of the maximum static load; although the failure was achieved at about 1800 cycles, rupture did not occur in weld bead as expected, but in base material (Fig. 11a).

It means probably that the two specimen edges were joined in an acceptable way. At the contrary, specimen no. 30 was tested at 35% of the maximum static load, and it reached the material stress limit at 2×10^6 showing the rupture in the weld (Fig. 11b). The trend presents the typical Wöhler curve behaviour with a decreasing load limit as a function of number of cycles up to failure. More tests may define accurately the fatigue limit for design purpose, but it can be ascertained that the behaviour of CDW Al joints is structurally reliable, provided that loading conditions are restricted well below the weld ultimate limit statically calculated.

3.5 Residual stress measurements

The residual stress measurements were performed, by means of the hole-drilling method, according to ASTM E837-01 standards, on two joints welded using different welding parameters (listed in Table 2); a single measurement point was considered in proximity of the weld toe. RESTAN automatic system and rectangular rosettes 1-RY61-1.5/120S were used in the half-bridge configuration to compensate the possible thermal strain. An incremental through hole was drilled using an advancing speed of 0.1 mm/min with parabolic step distribution. The measurement points were chosen as near as possible to the weld toe. The stresses were calculated by means of the power series method in order to consider the non-uniformity of the strains in the thickness. The measurements were carried out on two specimens, 13 and 17, welded using different parameters in order to evaluate possible influence of welding parameters on residual stress value. In particular, specimen 17 was welded using the optimal parameters.

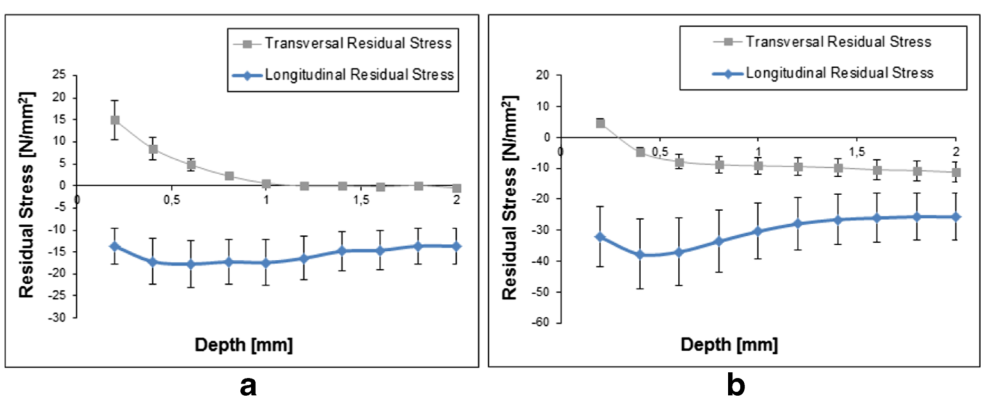

Fig. 12 Residual stress distribution measured on specimen 13 (**a**) and 17 (**b**)

Figure 12 reports the residual stress distribution in the thickness for specimens 13 and 17. Since the hole-drilling method is a semi-destructive technique, only one measurement can be carried out on each specimen. The error bar is included in the figure in order to show the typical scatter of this type of measurements. According to normal experimental practice, measurement errors have been evaluated on the basis of the considerations reported in [14, 15].

Measurement results showed that the CDW welding originated a very low residual stress field contrarily the traditional and friction stir welding process [16, 17]. In particular, low residual stress was originated in the weld axis direction, probably due to the compressive load applied during the welding. Moreover, it can be observed that the residual stress value was lower in the specimen 17 obtained using optimal welding parameters.

4 Conclusions

This work represents a further forward step in the study of an innovative welding technique such as CDW, in its multipoint variant on aluminium alloys.

In particular, several joints of rectangular section in aluminium alloy 5754 technique were realised using the multipoint capacitor discharge welding (MCDW) with a different set-up, and the optimal procedure consists in two heats and a series of discharges which reach the high energies more quickly.

Subsequent ultrasonic testing has largely confirmed the assumptions developed by visual inspection of the specimens, coupled with static tests; best results have been achieved for specimen 33, characterised by good weld shape and limited and acceptable extension of defects.

Fatigue tests and residual stress measurements were finally performed to verify the reliability of the welds, expressing the innovative application of MCDW process on aluminium alloy, which shows good potential development for future applications.

References

1. Venkataraman S, Devlietan JH (1988) Rapid solidification of stainless steels by capacitor discharge welding. Weld J Res Suppl 67: 111–118
2. Alley RL (1991) Capacitor discharge stud welding. ASM handbook vol.6: welding, brazing and soldering. American Welding Society, USA
3. Dattoma V, Palano F, Panella FW (2010) Mechanical and technological analysis of AISI 304 butt joints welded with capacitor discharge process. Mater Des 31:176–184
4. Chiozzi S, Dattoma V, Panella FW (2008) Capacitor discharge welded bars of Inconel 718 and TiAl6V4 superalloys under fatigue. Mater Des 29:839–851
5. Palano F, Panella FW, Dattoma V (2010) Characterization of aeronautical engine parts joined by CDW welding process. P I Mech Eng G-J Aer 223:11–22
6. Li Z, Hao C, Zhang J, Zhang H (2007) Effects of sheet surface conditions on electrode life in resistance welding aluminium. Weld J Res Suppl 86:81–89
7. Palano F, Chiozzi S, Panella FW, Dattoma V (2012) Characterization of steel welded joints with hybrid projection and capacitor discharge welding (CDW) processes. Mater Manuf Process 27:1387–1391
8. Green RE Jr (1986) Ultrasonic non-destructive materials characterization. NASA Lewis Research Center Analytical Ultrasonics in Materials Research and Testing, New Jersey 1–29 (SEE N86–22962 13–38)
9. Spinella DJ, Brockenbrough JR, Friday JM (2005) Trends in aluminium resistance spot welding for the auto industry. Weld J 84:34–40
10. Ronnhult T, Rlby U, Olefjord I (1980) The surface state and weldability of aluminium alloys. Mater Sci Eng A 42:329–336
11. Panella FW, Casalino G (2006) Numerical simulation of multipoint capacitor discharge welding of AISI 304 bars. Proc IMechE Part B J Eng Man 220:647–655
12. Sasaki K, Kishida M, Itoh T (1997) The accuracy of residual stress measurement by the hole-drilling method. Exp Mech 37(3):250–257
13. Ottel R (2000) The determination of uncertainties in residual stress measurement (using the hole drilling technique), Standard measurement & testing project no. SMT4-CT97–2165, Issue 1
14. De Giorgi M, Scialpi A, Panella FW, De Filippis L (2009) Effect of shoulder geometry on residual stress and fatigue properties of AA6082 FSW joints. J Mech Sci Technol 23:26–35
15. Dattoma V, De Giorgi M, Nobile R (2009) On the residual stress field in the Aluminium alloy FSW joints. Strain 45:380–386
16. Panella FW, Casalino G (2007) Microsructural analysis of AISI 304 bars welded with high speed pulsed discharges. J Mater Process Technol 191:149–152
17. Han L, Thornton M, Boomer D, Shergold M (2010) Effect of aluminium sheet surface conditions on feasibility and quality of resistance spot welding. J Mater Process Technol 210:1076–1082